Article

Not peer-reviewed version

Structure-Function and Treg induction of Methylated CpG ODNs from *Bifidobacterium longum* susp. *infantis* in an Allergic Murine Model

Dongmei Li , Idalia Cruz , Samantha Peltak , Patricia L. Foley , Joseph Bellanti *

Posted Date: 20 June 2025

doi: 10.20944/preprints202506.1691.v1

Keywords: methylated CpG; oligonucleotides; Treg; IL-10; OVA-allergenic murine model

 doi:10.20944/preprints202506.1691.v1

Article

Structure-Function and Treg induction of Methylated CpG ODNs from *Bifidobacterium longum* susp. *infantis* in an Allergic Murine Model

Dongmei Li [1], Idalia Cruz [2], Samantha Peltak [1], Patricia L. Foley [2] and Joseph A. Bellanti [1,3,*]

[1] Department of Microbiology & Immunology, Georgetown University Medical Center, Washington, D.C. 20057

[2] Department of Oncology, Animal Models, Shared Resources, Georgetown University Medical Center, Washington, D.C. 20057

[3] Department of Pediatrics, Georgetown University Medical Center, Washington, D.C.20057

* Correspondence: bellantj@georgetown.edu

Abstract

In our previous studies, methylated CpG oligodeoxynucleotides (ODN) derived from *Bifidobacterium longum* subsp. *infantis* have demonstrated immunomodulatory activity through the induction of regulatory T cells (Tregs). To define the structural determinants underlying this effect, we synthesized four CpG ODNs varying in methylation status, CpG motif placement, and backbone length. These include: 1) ODN-A (2m-V1), a 20-nucleotide CpG oligodeoxynucleotide incorporating two 5-methylcytosines at positions 4 and 12 within centrally placed CpG motifs; 2) ODN-B (um-V2), a 20-nucleotide CpG oligodeoxynucleotide with a backbone structure identical to ODN-A but unmethylated; 3) ODN-C (2m′-V3), a 20-nucleotide CpG oligodeoxynucleotide with a backbone structure identical to ODN-A, with two 5-methylcytosines shifted at positions 7 and 15; 4) ODN-D (3m-V4), a 27-nucleotide CpG oligodeoxynucleotide with an extended backbone structure, with three 5-methylcytosines at positions 3, 11 and 19.Using a murine model of OVA-induced allergy, we show that methylated ODN-A (2m-V1) and ODN-D (3m-V4) markedly reduced serum anti-OVA IgE, clinical symptoms, eosinophilic infiltration, and Th2/Th17 responses, while promoting splenic Treg expansion and IL-10 production. In contrast, unmethylated ODN-B (um-V2) and a positionally altered methylated ODN-C (2m′-V3) failed to suppress allergic inflammation, reversely enhanced Th2/Th17 response, and induced in vitro robust TLR7/8/9 expression in native splenocytes. These findings suggest that both methylation and motif architecture critically influence the immunologic profile of CpG ODNs. Our results provide mechanistic insights into CpG ODN structure–function relationships and support the therapeutic potential of select methylated sequences for restoring immune tolerance in allergic disease.

Keywords: methylated CpG; oligonucleotides; Treg; IL-10; OVA-allergenic murine model

1. Introduction

Allergen-specific immunotherapy (AIT) is currently the only curative treatment available for allergic diseases that has long-term efficacy. The immunomodulatory properties of DNA, particularly synthetic and microbial-derived oligodeoxynucleotides (ODNs) used as immune conjugate, have garnered increasing interest as a strategy to treat a wide variety of diseases, including cancers, infections [1,2] and recent allergic diseases[3,4]. Among these, CpG-containing ODNs are of particular interest that can be used either as a standalone molecule or as an adjuvant to modulate innate and adaptive immunity through Toll-like receptor 9 (TLR9) signaling [5]. However, while unmethylated CpG motifs typically promote immune activation and are being developed as vaccine

 doi:10.20944/preprints202506.1691.v1

adjuvant for cancer immunotherapy [6,7], certain CpG ODNs such as TLR-9 antagonist CpG-c41[8,9] exert immunosuppressive or tolerance-inducing effects. Apparently, influence on innate and adaptive immunity depends on CpG-containing DNA sequence context, methylation status, and epigenetic structural features [5,10,11].

Using CpG ODN therapies to restore immune tolerance in allergic and autoimmune diseases is the primary focus of our work [12]. Building on this growing body of evidence, our group reported that genomic DNA from *Bifidobacterium longum* subsp. *infantis* selectively induces Foxp3⁺ regulatory T cells (Tregs) from human peripheral blood mononuclear cells in vitro [13]. In the same study, methylome sequencing identified a unique methylated m5C-containing CpG motif in this probiotic strain. A synthetic CpG ODN derived from this methylated motif demonstrated potent Treg-inducing activity in vitro. These findings were further validated in vivo using a murine model of allergic inflammation, where administration of the methylated CpG ODN attenuated inflammatory symptoms, reduced Th2 cytokine levels in serum, decreased mast cell infiltration at the injection site, and enhanced the differentiation of splenic Foxp3⁺ Tregs[14]. A subsequent dose–response study confirmed that the Treg-promoting effect was dose-dependent and preferentially associated with the methylated, rather than the unmethylated, form of the ODN [15]. Together, these findings highlight the therapeutic potential of probiotic-derived methylated CpG motifs for modulating immune responses in both hypersensitivity and systemic lupus erythematosus (SLE)[16].

While these results support the therapeutic potential of methylated CpG ODNs, the molecular basis for their differential activity remains undefined. In particular, the contribution of specific structural elements, such as the number and position of methyl groups, backbone length, and CpG spacing, to their immunoregulatory function has not been systematically studied.

In the present work, we investigate the structure-function relationships of a panel of synthetic CpG ODN variants derived from the native *Bifidobacterium longum* subsp. *infantis* sequence. We hypothesized that defined modifications in methylation and backbone architecture would differentially impact their ability to induce Foxp3⁺ Tregs and modulate allergic inflammation. Using a murine model of ovalbumin (OVA) allergy, we analyzed immunologic endpoints including Treg differentiation, cytokine profiles, serum specific anti-IgE level and histopathologic inflammation.

Our results identify key structural determinants of CpG ODN–mediated immune regulation and offer mechanistic insights into the rational design of nucleic acid–based immunotherapies for allergic disease.

2. Materials and Methods

2.1. Synthetic Short-Chain Oligodeoxynucleotides (ODNs), Allergen OVA and Immunoadjuvant:

Four synthetic ODNs were used in this study, which are synthesized by Integrated DNA Technologies. As shown in Figure 1A, the sequences 2m-V1 is 20-bp in length, with the DNA sequence as 5′-C*A*G*/iMe-dC/GGCGCCG/iMe-dC/GGCGC*C*T*G, containing a duplicate of the Bl-T2 m5C motif [(A/G) GCpGGCGCC)] of *B. longum* subsp. *infantis* [14]. The unmethylated counterpart, um-V2 (5′-C*A*G*CGGCGCCGCGGCGC*C*T*G), mirrors 2m-V1 without methylation. The new synthesized 2m′-V3 share the same sequence of 2m-V1 but with different methylated CpG location and 3m-V4 is designed to contain a triplicate of B1-T2 motif (Figure 1). All four ODNs feature a nuclease-resistant phosphorothioate backbone in first and last three nucleotides, as indicated by "*"in the Figure 1A.

Lyophilized form ODNs was dissolved in PBS as 3 mg/mL and kept at -20ºC until use. Predicted secondary structure stability, accessed via Gibbs free energy (ΔG), revealed ΔG values of −11.3 kcal/mol for both 2m-V1 and 2m′-V3, and a less negative ΔG of −9.3kcal/mol for um-V2, suggesting reduced structural stability in the unmethylated form. 3m-V4 is an extended version of the BI-T2 motif, consisting of 27 nucleotides with three methylated cytosine(s). Its ΔG value, calculated without phosphorothioate (PTO) and methylation modifications, was −20.3kcal/mol. When PTO and

 doi:10.20944/preprints202506.1691.v1

methylation were included, ΔG further decreased to −21.8 to −22.8kcal/mol, indicating the highest thermodynamic stability among the four ODNs.

The immunogenic low- endotoxic OVA (ovalbumin) was purchased from Chondrex, Inc (WA, USA) with endotoxic level <1 EU/mg. A stock solution was made by dissolving 10 mg lyophilized form was dissolve in 1 mL of sterile PBS and stored in a -20ºC until it is used. Immuno adjuvant AddaVax was purchased from InvivoGen (SanDiego,USA). This ready-to-use form of adjuvant is a squalene-based nanoemulsion and stored at 4ºC. We mixed AddaVax with different doses of the allergens OVA with or without ODN that pre-prepared in PBS at 1:2 ratio. A aliquot of 100μL such mixture per mouse was then sterilized by filtering through a 0.2 μm filter just before the subcutaneous injection.

2.2. Animals and Groups

Female BALB/c mice aged 6-8 weeks were sourced from Jackson Laboratory (Bar Harbor, ME) and housed in autoclaved plastic cages on individually ventilated racks at 70-74°F in Georgetown University Division of Comparative Medicine (DCM). Mice were fed 5053 - PicoLab Rodent Diet 20 (LabDiet, St. Louis, MO) that contains 20% protein without peanut and egg protein. The procurement occurred one week before the initiation of the experiment, allowing the mice a crucial acclimatization period within the DCM environment. During this period and entire experiment, the mice had access to food and water ad libitum, residing in a ventilated caging cabinet (< 5) with environmental conditions including a 12-hour light-dark cycle, humidity levels between 60-80%. Stringent ethical standards, in accordance with guidelines set forth by the Association for Assessment and Accreditation of Laboratory Animal Care International (AAALAC) and the Institutional Animal Care and Use Committee (IACUC) of Georgetown (Protocol #2022-0021), were strictly adhered to throughout the study.

A total of 30 mice were organized into six groups (group Ato group F) with 6 mice in each group except 3 mice for Group A (PBS+AddaVax vehicle control) and Group F. Group B mice were subcutaneously injected with OVA only (Allergic condition induction control), and oligodeoxynucleotides treated mice groups by additional 2m'-V3 in Group C, 3m-V4 in Group D, um-V2 in Group E, and 2m-V1 in Group F.

2.3. OVA Sensitization and Challenge Model

Allergic model followed previous report [14] and the injections as scheduled in Figure 1B. Briefly, allergen OVA in 20 μg/mouse was introduced in Day 1 and Day 8 to sensitize the mice except mice in Group A, and 200μg on Day21 to challenge the mice. OVA alone or with 100μg ODN in PBS was mixed with adjuvant AddVax in 2:1 ratio to subcutaneously inject in the middle part of back area that had been shaved prior to the first injection. This mixture was prepared fresh on injection day, and passed through a 0.2 μm syringe filter to ensure it is sterile. On day -1, baseline blood samples were drawn from three mice in each group for measurement of serum IgE concentrations. The clinical symptoms observed within 1 hour after antigen challenges were recorded and all the mice were euthanized on Day 22. Blood and spleen specimens were collected and 1.5 cm x 1.5 cm skin biopsy specimens were taken at the injection site.

2.4. Measurement of Serum Anti–OVA-IgE and Clinical Symptom

Serum concentrations of anti–OVA specific IgE were determined using a mouse anti-OVAIgE antibody ELISA kit (Catalog #3004; Chondrex Inc, Woodinville, WA), following the manufacturer's instructions. Clinical symptoms were assessed 1 hour after the OVA challenge on Day 21, using a scoring system as previously described [14] as follows: 0: No evident symptoms; 1–2: Mild to intermediate symptoms (e.g., scratching and rubbing of the nose and head or intention on the injected site on the back, with fore limbs or hind limbs, edema around the eyes and mouth); and 3: Severe symptoms (e.g., labored breathing, tremors, or major respiratory distress).

 doi:10.20944/preprints202506.1691.v1

2.5. Histopathology and Eosinophils Percentage

Skin tissues from the injection sites were collected, fixed in 10% formalin, embedded in paraffin, and sectioned at 5 μm for hematoxylin and eosin (H&E) or Giemsa staining. Stained sections were scanned and evaluated for the severity of inflammation. Eosinophilic inflammation was also quantified by counting eosinophils within the inflammatory infiltration area, using skin samples from three mice per group.

Eosinophil quantification was performed by examining five 40× fields per section. In each field, the percentage of eosinophils was calculated relative to the total number of infiltrating cells (excluding epithelial cells) in ImageJ program. These percentages were then compared across treatment groups to assess differences in eosinophilic inflammation.

2.6. T-Cell Phenotypes in Spleen by Flow Cytometric Analysis

On Day 22, spleens were harvested from mice, homogenized, and passed through a 40-μm cells trainer to prepare single-cell suspensions. Red blood cells (RBCs) were lysed using 3mL of cold RBC Lysis Buffer (Thermo Fisher Scientific). Splenocytes were then washed with cold complete RPMI medium by centrifugation at 1600 rpm for 10 minutes at 4°C. Cell viability was assessed using 0.2% trypan blue.

T-cell subsets within the splenocytes population were identified using 10 fluorochrome-conjugated antibodies. CD45R/B220 was used to define the B-cell population. For surface staining, 2 × 10^6 splenocytes per well were plated in 96-well plates in 200 μL aliquots. After two washes, cells were stained with Zombie R718 viability dye (BioLegend; 1:500 dilution) for 15 minutes at room temperature. Surface staining was performed using fluorochrome-conjugated anti-mouse antibodies (BioLegend), including CD3BV605 (clone 17A2), CD4BV785 (cloneGK1.5), CD25APC-Cy7 (clonePC61.5), and CD45R/B220 (clone RA3-6B2).

For intracellular staining, cells were fixed and permeabilized using the Intracellular Staining Fixation Buffer and Perm/Wash Buffer set (BioLegend). Intracellular markers were stained in Perm/Wash Buffer using the following fluorochrome-conjugated antibodies (BioLegend), including anti-Tbet BV421 (clone 4B10), GATA3 PerCPCY5.5 (clone 16E10A23), FOXP3 AF488 (clone MF-14), IFN-γ PE/Dazzle 594 (clone XMG1.2), IL-4 BV711 (clone 11B11/BVD6-24G2), IL-17APE (clone TC11-18H10.1), and IL-10 APC (clone JES5-16E3). Flow cytometric analysis was performed using a BD Fortessa SORP (BD Biosciences), and data were analyzed with FCS Express 7 (DeNovo Software). Each fluorochrome-conjugated antibody was compensated using Compensation Beads (BioLegend). Fluorescence Minus One (FMO) controls were included for each antibody in every experiment. Treg cells ($CD25^+FOXP3^+$), Th1 ($IFN\gamma^+T\text{-}bet^+$), Th2 ($IL\text{-}4^+GATA3^+$), and Th17 ($IL\text{-}17A^+CD4^+$) populations were gated from viable $CD3^+CD4^+$ T cells, as outlined in the gating strategy shown in Figure S1.

2.7. Serum Cytokine Responses in ODN-Treatedmice

Mouse serum was collected from whole blood by centrifugation at 2000 rpm for 10 minutes at 4°C. Serum samples were stored at -80°C until use. Cytokine concentrations were measured using the LEGENDplex™Multi-Analyte Flow Assay Kit (BioLegend), specifically the mouse Th1/Th2 Panel(8-Plex), following the manufacturer's instructions. The panel included IFN-γ, IL-5, TNF-α, IL-2, IL-4, IL-6, IL-10, and IL-13. Total TGF-β1 and IL-10 levels were additionally quantified using the BioLegend MAX™ Total TGF-β1 ELISA Kit and IL-10 ELISA Kit, respectively.

2.8. In Vitro Splenocytetlr7,TLR8, andTLR9 TRANSCRIPTION

Two million splenocytes isolated from PBS-control mice (Group A) were washed twice with complete RPMI 1640 medium and resuspended in 0.5 mL medium in a 24-well plate. Cells were treated with 25 μg of 2m-V1 (methylated oligo), um-V2 (unmethylated oligo), or 2m'-V3 (methylated oligo) dissolved in 50 μL PBS. Control wells received 50 μL PBS without ODNs. Plates were incubated at 37°C in a 5% CO_2 atmosphere for 2 or 6 hours. Treated splenocytes were harvested at 2h or 6 hours

 doi:10.20944/preprints202506.1691.v1

for RNA extraction using TRIzol reagent (Invitrogen). RNA purity was confirmed by an A260/A280 ratio between1.8 and 2.0. Reverse transcription was performed using the High-Capacity cDNA Reverse Transcription Kit (Applied Biosystems). Quantitative PCR was conducted using SYBR Green PCR Master Mix (Applied Biosystems) to assess the expression of TLR7, TLR8, and TLR9, with the following primer sets: TLR7 Forward(5′-CATCTGTCTTTGCCCCTCTAAG) and Reverse (5′-AGTTTCTTGACCTGTGCCTC); TLR8 Forward (5′-GAGTTCCTTGAGCTGTTTGC) and Reverse (5′-ACTTCCTTTTCTGTGTACCCC); TLR9 Forward (5′-AGAGGAAGAGAAAGTGGGAGAG) and Reverse (5′-AGGACACAGAACCAGGACTAG); and internal control primers for MGADPH Forward (5'-TTCACCACCATGGAGAAGGC) and MGADPH Reverse (5'-AGTGATGGCATGGACTGTGG),

2.9. Statistical Analysis

Continuous variables are expressed as the means ± standard deviation (SD), and categorical data are presented as frequencies or percentages. We performed the student's t-test (comparing the two groups) and one-way ANOVA (comparing three or more groups), followed by Tukey's (comparing all groups) or Dunnett's (comparing treatments vs. control) post-tests to assess the significance of changes relative to controls as indicated. All statistical analyses used 2-sided tests and a p value≤ 0.05 was considered significant. All tests were performed with the GraphPad Prism10.0 (San Diego, USA).

3. Results

To evaluate the immunologic consequences of structural modifications in CpG ODNs, we tested four synthetic variants that differed in methylation status, CpG motif positioning, and backbone length (Figure 1A). For ODN nomenclature, the prefix number indicates the number of methylated cytosine residues. For example, "2m" in 2m-V1 and "3m" in 3m-V4 correspond to two and three methylated cytosine(s), respectively, while "um" in um-V2 refers to an unmethylated ODN. The designation 2m'-V3 indicates two methylated cytosine(s) located at alternative positions compared to naïve Bifidobacterium methylated motif. The "V" denotes "vaccine," and the accompanying number reflects the chronological order in which the variants were designed. A murine model of ovalbumin (OVA)-induced allergic inflammation was used to assess the in vivo immunological effects of co-treatment with each CpG ODN variant (Figure 1B). Key outcome measures included serum IgE levels, clinical allergy scores, tissue histopathology, frequencies of regulatory T cells (Tregs) and effecter T cells (Teff), cytokine profiles, and expression levels of nucleic acid-sensing Toll-like receptors (TLRs).

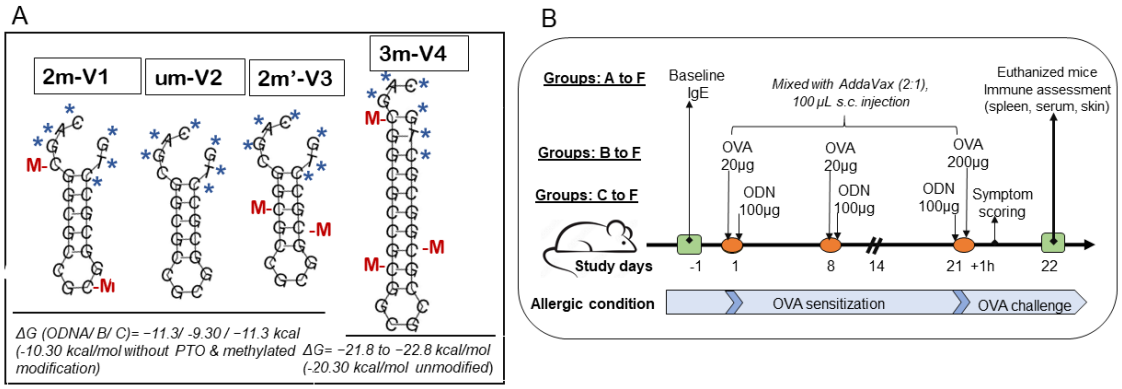

Figure 1. Secondary structures of four CpG oligodeoxynucleotides (ODNs) and experimental timeline for mouse allergy model. (A) The four CpG ODNs were designed based on the methylated cytosine-containing BI-T2 motif (RGCGGCGCC) derived from Bifidobacterium longum subsp. infantis. 2M-V1 is a 20-mer sequence containing two methylated cytosine(s) ("M", shown in red) located according to the native m5C motif. UM-V2 is the unmethylated version of 2M-V1, while 2M'-V3 includes methylated cytosine(s) at alternate positions. All

 doi:10.20944/preprints202506.1691.v1

three share identical base sequences but differ in methylation pattern. 3M-V4 is an extended version of the BI-T2 motif, comprising 27 bases with three methylated cytosine(s). "M" indicates methylated cytosine residues, and "*" denotes phosphorothioate backbone modifications. (B) Timeline of the animal study over a 22-day period. A total of 30 female BALB/c mice (6–8weeksold)were randomly divided into six groups. Ovalbumin (OVA)-induced allergy was established by subcutaneous sensitization with 20μg OVA on Days 1 and 8, followed by a challenge with 200μg OVA on Day 21. Group B received OVA alone and served as the allergic control. Groups C–F were co-treated with OVA and one of the four ODNs: Group C (2m'-V3), Group D(3m-V4), GroupE (um-V2), and Group F(2m-V1), to assess their immunomodulatory potential under allergic conditions. Groups A (PBS vehicle control) and F (2m-V1, known positive immunomodulator) each contained 3 mice. Group B and selected ODN groups (C–E) included 6 mice, with emphasis placed on comparisons involving unmethylated um-V2, methylated 2m'-V3, and 3m-V4. Clinical allergy symptom scores were assessed 1 hour post-OVA challenge. Spleen, serum, and skin tissues at the injection sites were collected on Day 22 following euthanasia.

3.1. Methylated 3m-V4 and 2m-V1 Suppress Serum Anti-OVA IgE Levels and Allergic Symptoms

Serum levels of OVA-specific IgE were measured on Day 22, a 24 hours after the OVA challenge. As expected, OVA challenge after 2-weeks sensitization significantly elevated anti-OVA IgE levels in mouse sera. However, this increase was effectively suppressed in mice when co-treated with methylated 3m-V4 and 2m-V1 (Figure 2A). In contrast, mice receiving unmethylated um-V2 or positionally altered methylated 2m'-V3 maintained high levels of serum IgE.

Consistent with the elevated IgE levels, allergic symptom scores at a day earlier (1 hour post the OVA challenge on Day 21) varied in different ODN-co-treated groups. After a 200 μg OVA challenge, the severity of allergic symptoms, measured by the frequency of scratching (using front or rear legs) and scratching area (ear and or subcutaneously injected back), was significantly higher in the OVA-alone and OVA + um-V2 treated mice (Figure 2B). These allergic symptoms were less manifested in mice group receiving the co-treatment with methylated ODNs, particularly 2m-V1 and 3m-V4.

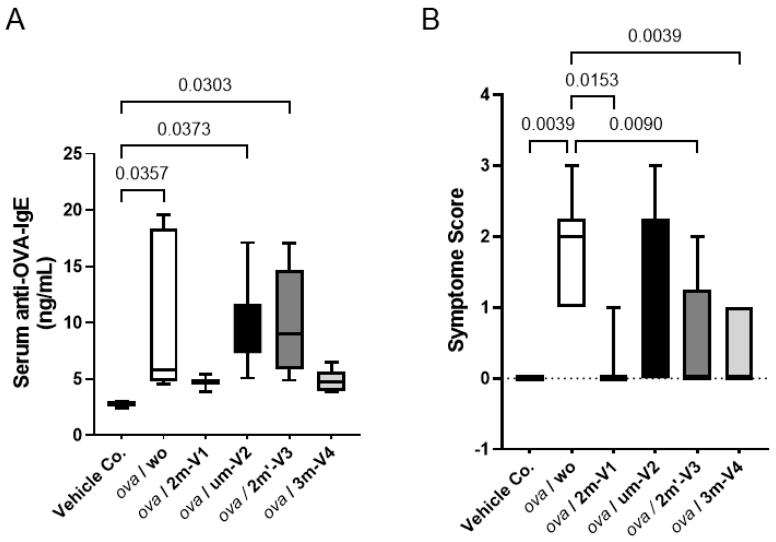

Figure 2. Serum anti-OVA IgE concentrations and clinical allergy symptom scores. (A) Serum levels of OVA-specific IgE (ng/mL) were quantified by ELISA from samples collected on Day 22. All 30 mouse serum samples were analyzed in duplicate. Bracket bars indicate pairwise group comparisons. The vehicle control group received PBS and AddaVax adjuvant. "ova/wo" denotes the allergic group treated with OVA alone, while "ova/ODNs" represents groups co-treated with OVA and one of the four ODNs. Notably, methylated 3m-V4 and 2m-V1 significantly reduced serum IgE levels compared to OVA-only controls, whereas unmethylated um-V2 (ova/um-V2) and alternatively methylated 2m'-V3 (ova/2m'-V3)failed to suppress IgE production. (B)

 doi:10.20944/preprints202506.1691.v1

Median clinical symptom scores were assessed 1 hour after OVA challenge for each group. OVA-induced allergic symptoms were markedly alleviated by co-treatments with methylated 2m-V1, 2m'-V3, and 3m-V4, but not by unmethylated um-V2. Statistical significance ($p<0.05$) is indicated for relevant group comparisons.

3.2. Methylated 3m-V4 and 2m-V1 Partially or Fully Restore the OVA-Induced CD4+ Reduction

On Day 22, the proportion of viable splenocytes in the vehicle control group (PBS–AddaVax–treated mice) remained high at 85.26%, with only minor changes observed across most treatment groups (Figure 3A). In contrast, OVA-challenged mice without any CpG ODN treatment (ova/wo) exhibited a significant reduction in splenocytes viability, by dropping to 81.86% ($p < 0.05$). This decline was mitigated by co-administration of any of the four CpG ODN variants tested. Among them, 3m-V4 and 2m-V1 demonstrated a stronger protective effect compared to the unmethylated um-V2 and the positionally methylated 2m'-V3. Notably, there were no statistically significant differences in splenocytes viability between any of the OVA+ODN treatment groups and the PBS control, suggesting that these CpG ODNs not only lack cytotoxic effects but may also confer a degree of protection against OVA-induced immune cell stress.

Different from cell viability, the $CD4^+$ T cell population in the spleen varied depending on the specific ODN used (Figure 3B). Consistent with reduced cell viability, $CD4^+$ cell frequency was significantly decreased in OVA-challenged mice compared to controls ($p<0.001$). Co-injection with 2m-V1 or 3m-V4 effectively prevented this reduction, showing statistically significant restoration of $CD4^+$ cells when compared to the ova/wo group ($p < 0.05$ and $p < 0.0001$, respectively). In contrast, unmethylated um-V2 and positionally methylated 2m'-V3 failed to restore $CD4^+$ cell levels, indicating that their ability to counteract OVA-induced $CD4^+$ reduction was limited.

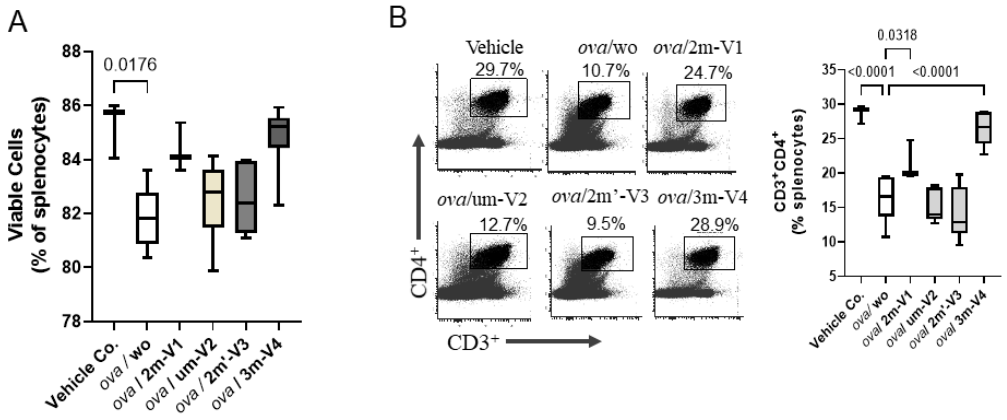

Figure 3. OVA challenge suppresses $CD4^+$ T cells and reduces splenic cell viability. BALB/c mice (n = 3–6 per group) underwent a 3-week treatment regimen as outlined in Figure 1B, followed by spleen harvest on Day 22. Splenocytes were isolated and analyzed via flow cytometry. Gating strategies for identifying conventional $CD4^+$ T cells and subsets are provided in Supplementary Figure S1. (A) OVA challenge (ova/wo group) significantly reduced the number of viable splenocytes compared to vehicle control. Co-treatment with methylated 2m-V1 or 3m-V4 partially or fully restored splenic cell viability. (B) Representative flow cytometry plots show the percentage of $CD3^+CD4^+$ T helper cells in each treatment group. OVA- induced depletion of $CD4^+$T cells was notably prevented by co-treatment with 2m-V1 or 3m-V4, resulting in levels comparable to vehicle controls. Bar graph displays median group values, with statistical comparisons performed by one-way ANOVA. Significant differences ($p<0.05$) are indicated; non-significant comparisons are unlabeled.

3.3. Methylated 3m-V4 and 2m-V1 Increase Treg Cells and Reduce Th2 and Th17 Subsets in OVA-Challenged Mice

 doi:10.20944/preprints202506.1691.v1

Despite the overall reduction in the $CD4^+$ T cell population, the percentage of Treg cells in OVA-challenged mice was slightly higher than in the negative control group, though this difference was not statistically significant. Co-administration of each ODN with OVA further increased the proportion of splenic Treg cells ($CD25^+FOXP3^+$) (Figure 4A), including significant increases in the um-V2 (p=0.0025) and 2m'-V3 (p=0.0182) groups compared to the PBS control. Importantly, when compared to the OVA-challenged group, Treg percentages were significantly elevated in mice treated with 3m-V4 (p = 0.023) and 2m-V1 (p = 0.01). Together with their higher total $CD4^+$cell counts, these findings strongly support a Treg-promoting effect of 3m-V4 and 2m-V1in OVA-challenged mice.

To examine how this regulatory T cell response aligns with effecter T cell (Teff) activity, we analyzed Th2 ($GATA3^+IL\text{-}4^+$), Th17 ($CD4^+IL\text{-}17^+$), and Th1 ($T\text{-}bet^+IFN\text{-}\gamma^+$) populations as well. As shown in Figure 4B, OVA-challenged mice exhibited a pronounced increase in Th2 cells. This elevation was significantly suppressed by co-treatment with methylated 3m-V4 (p = 0.0039), while 2m-V1 showed a similar trend that did not reach significance. In contrast, co-treatment with unmethylated um-V2 significantly increased Th2 frequency compared to the OVA-only group (p = 0.0017), suggesting a possible exacerbation of Th2 inflammation. A slight, non-significant increase in Th2 cells was also observed in the 2m'-V3 group. Regarding the Th17 response (Figure 4C), unmethylated um-V2 was the only condition that significantly elevated Th17 levels compared to OVA alone mice. In contrast, the Th1 population (Figure4D) remained unchanged across all treatment groups, including PBS controls, OVA-challenged mice, and those co-treated with various ODNs.

The overall immune responses in each group were then evaluated by their Treg/Teff ratios. The Treg/Th2 ratio was significantly decreased in OVA-only mice compared to the PBS control (p = 0.034) as expected, indicating a shift toward pro-allergic inflammation. This imbalance was effectively corrected by 3m-V4 co-treatment (p = 0.006). In contrast, the elevated Th2 responses in um-V2 and 2m'-V3 groups maintained a lower Treg/Th2 ratio. Compared with the Treg/T2 ratio, the Treg/Th17 ratio was less affected in OVA-only mice, but a pronounced reduction was observed in the OVA/um-V2 group, which showed elevated Th17 levels. Remarkably, the 3m-V4 group displayed both higher Treg levels and significantly suppressed Th17 responses, demonstrating by its significantly higher Treg/Th17 ratio compared to OVA-only mice.

Taken together, these results suggest that 3m-V4, and to a lesser extent 2m-V1, can counteract OVA-induced Th2 and Th17-driven inflammation by promoting a strong Treg response. In contrast, unmethylated um-V2 and positionally modified 2m'-V3 either failed to restore immune balance or exacerbated the pro-inflammatory environment, thereby disrupting the equilibrium between Treg and effecter T cell subsets.

 doi:10.20944/preprints202506.1691.v1

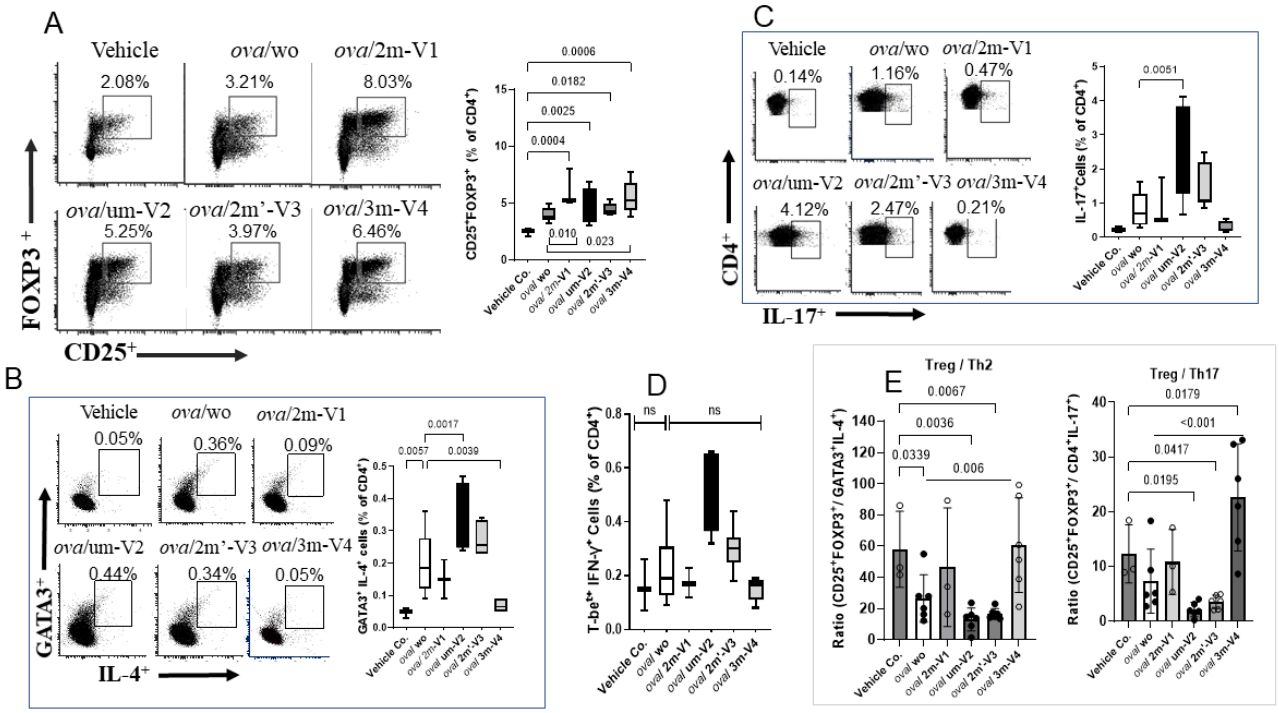

Figure 4. Flow cytometric analysis of T helper cell subset responses in mouse splenocytes from different treated groups. (A) The Treg subset ($CD4^+CD25^+FOXP3^+$) was elevated in all OVA-treated groups compared to vehicle controls. Co-treatment with methylated 3M-V4 or 2M-V1 further enhanced Treg expansion. (B) The Th2 subset ($CD4^+IL\text{-}4^+GATA3^+$) was significantly increased in OVA-challenged mice, with an even greater increase observed in the ova/um-V2 group. This Th2 expansion was effectively reduced in mice co-treated with 3m-V4. (C) A slight increase in Th17 cells ($CD4^+IL\text{-}17^+$) was observed in OVA-only mice, which was significantly amplified in the OVA + um-V2 group ($p = 0.005$). No significant changes were detected with other ODN treatments. (D) No significant differences were observed among groups in the Th1 subset ($CD4^+IFN\text{-}\gamma^+T\text{-}bet^+$). Bar graphs next to each flow plot show median values for each group. Statistical comparisons were performed using one-way ANOVA; significant differences ($p<0.05$) are indicated, while non-significant comparisons are not labeled.

3.4. Elevated IL-5 and IL-4 in um-V2 and 2m'-V3 co-Treated Mouse Sera Contrast to IL-10 Elevation in 3m-V4 and 2m-V1 Mice

Among the eight cytokines analyzed using the LEGENDplex™ Multi-Analyte Flow Assay Kit, IL-13 and IL-2 showed no significant differences between the treatment groups and the negative control (data not shown). The remaining six cytokines varied depending on the treatment group).

As shown in the top panel of Figure 5A, the Th2-related cytokine IL-4 was elevated in OVA-only mice compared to negative controls and further increased in the 2m'-V3 co-treated group. IL-5 levels were elevated in all OVA-treated groups, regardless of ODN co-treatment. However, co-treatment with unmethylated um-V2 or positionally altered methylated 2m'-V3 significantly increased serum IL-5 compared to PBS controls. The co-treatment with um-V2 showed the most pronounced effect, highlighting by significantly higher IL-5 levels in this group when compared to OVA-only group ($p = 0.001$). Similarly, the Th17-associated cytokine IL-6 was significantly elevated in the OVA + um-V2 group ($p = 0.01$), suggesting a potential synergistic inflammatory response driven by unmethylated um-V2.

Alongside with less Th1 cell phenotypes observed in spleen, the Th1-related cytokines were also affected. We observed that TNF-α in serum remained unchanged across all groups. However, IFN-γ level was significantly elevated in the OVA + 3m-V4 group compared to the negative control ($p = 0.0021$). A similar pattern was observed for IL-10 (Figure 5A, the bottom panel), which was also significantly increased in the OVA+ 3m-V4 group ($p = 0.017$).

 doi:10.20944/preprints202506.1691.v1

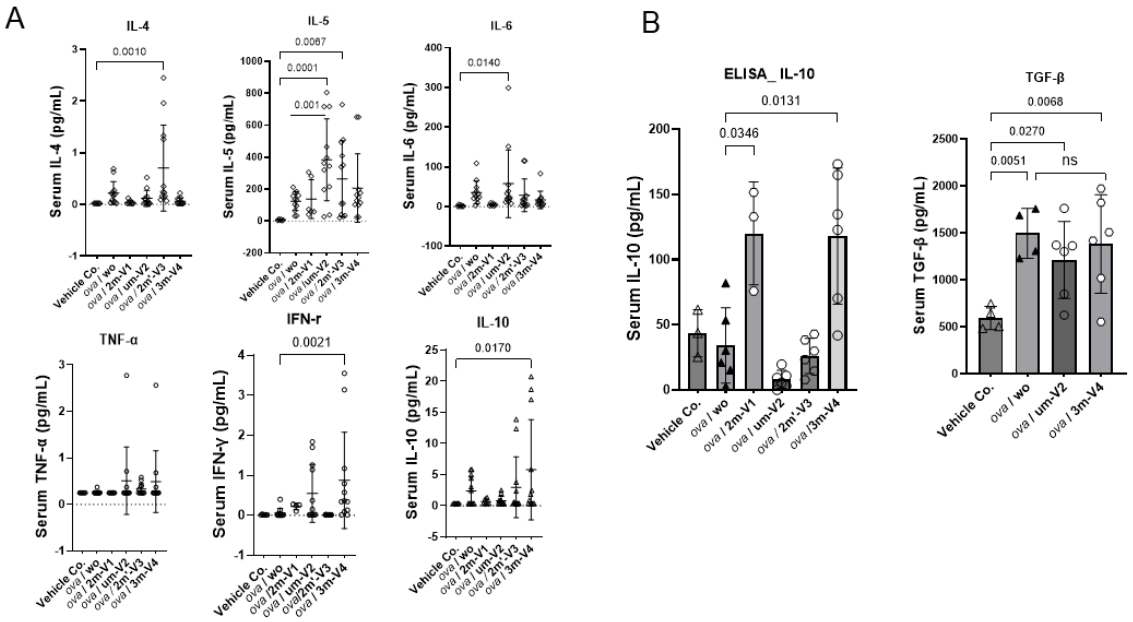

Figure 5. Serum cytokine responses to OVA and CpG ODN treatments. Cytokine levels were quantified using the LEGENDplex™ Multi-Analyte Flow Assay Kit(A),and ELISA assays (B). OVA treatment alone induced a heightened proinflammatory cytokine environment. Among the ODN co-treated groups, two distinct cytokine response patterns were observed. Unmethylated UM-V2 and alternatively methylated 2M'-V3 further amplified Th2-associated cytokines, including IL-4, IL-5, and Th17-associated IL-6, consistent with an exacerbated allergic profile. In contrast, co-treatment with methylated 3M-V4 or 2M-V1 shifted the cytokine milieu toward an immunoregulatory or tolerogenic state, as evidenced by elevatedIL-10 levels. Statistical comparisons were performed using one-way ANOVA; significant differences ($p<0.05$) are indicated, while non-significant comparisons are not labeled.

To validate the anti-inflammatory potential of methylated ODNs, we used ELISA to measure IL-10 across all treatment groups and TGF-β levels between the 3M-V4 and um-V2 conditions. As shown in Figure 5B, IL-10 levels were significantly elevated in OVA-challenged mice co-treated with methylated 2m-V1 and 3m-V4, with p-values of 0.03 and 0.01, respectively, compared to the OVA-only group. Consistent with our previous findings (Li, et al 2025b), TGF-β levels were not universally increased in response to OVA or ODN challenge, and neither um-V2 nor 3m-V4 altered this OVA-induced baseline.

Taken together, these cytokine profiles indicate that methylated ODNs, particularly 3m-V4, promote anti-inflammatory cytokine responses, potentially counteracting OVA-induced inflammation. Instead, unmethylated um-V2 and the positionally altered methylated 2m'-V3 appear to exacerbate the inflammatory response.

3.5. OVA-Induced Local Skin Inflammation is Exacerbated by Unmethylated um-V2 and Alternate Methylated 2m'-V3 with Elevated Serum IL-5 Response

Histopathologic changes at the injection site were evaluated by H&E staining. Inflammatory cell infiltration in the dermis was clearly observed in OVA-treated mice and was more pronounced in those co-treated with um-V2 or 2m'-V3 (Figure6A). Compared tothe OVA-alone group, where inflammation was more diffusely distributed throughout the dermal layer, the co-treatment with um-V2 or 2m'-V3 resulted in a more compact and denser band of inflammatory cells.

 doi:10.20944/preprints202506.1691.v1

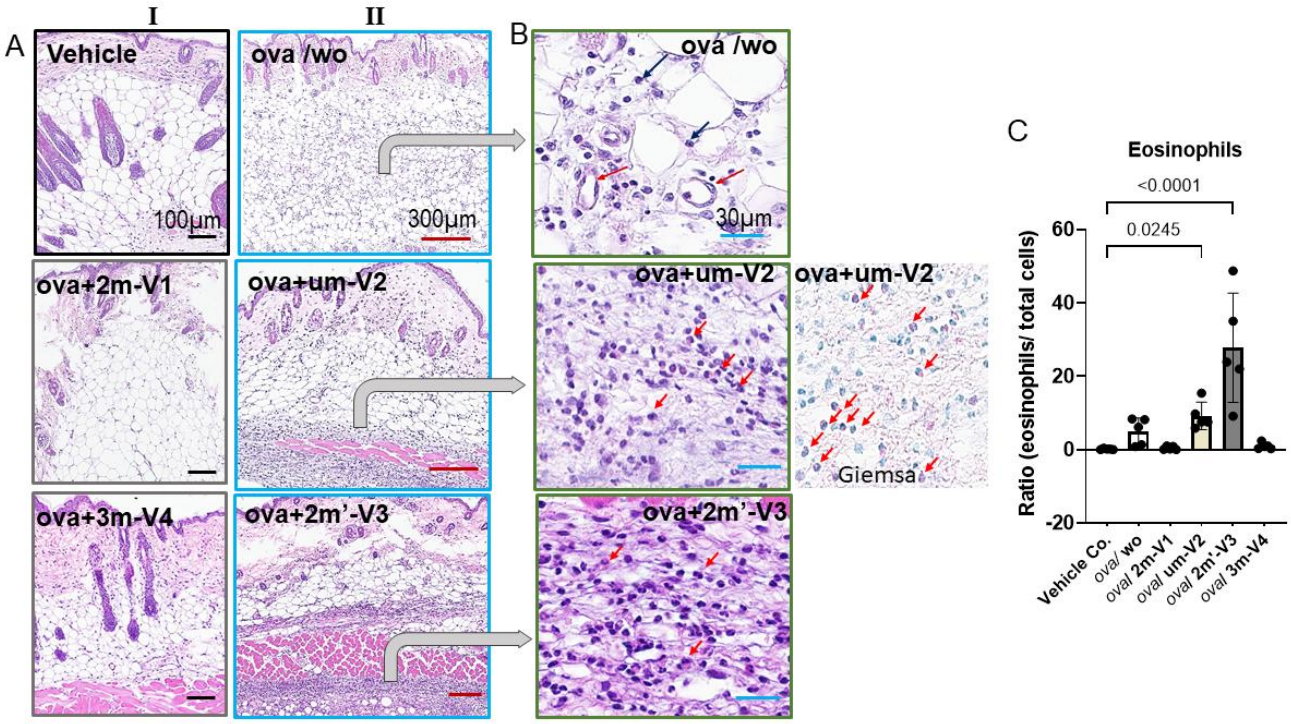

Figure 6. Histopathological evidence that methylated 2m-V1 and 3m-V4 alleviate OVA-induced skin inflammation. (A) Representative hematoxylin and eosin(H&E) images of skin tissue sections from each treatment group. In column I, light or no inflammatory response is seen in ova/2m-V1 and ova/3m-V4. Prominent inflammatory cell infiltrates are observed in the dermis and subcutaneous adipose layers of OVA-challenged mice (ova/wo), as well as in ova /um-V2 and ova/ 2m'-V3 groups (II column). While ova/wo mice exhibit more diffuse infiltration, the presence of um-V2 and 2m'-V3 results in a denser and more band-like pattern of infiltrates. (B) Enlarged views of H&E and Giemsa-stained sections highlight abundant eosinophils infiltration (indicated by red arrows) in ova /um-V2 and ova/ 2m'-V3 mice, characterized by red granularcytoplasm. In contrast, infiltrates in the OVA-only group are predominantly mononuclear cells (black arrows) localized around dilated capillaries. Scale bars are indicated at the top of each image column. (C) Quantitative comparison of eosinophil proportions within the inflammatory infiltrate across groups. The OVA + um-V2 and OVA + 2m'-V3 groups show significantly higher eosinophil recruitment, likely driven by their elevated IL-5 response.

Two predominant cell types were identified within the infiltrates. The first type consisted of small, round cells with dense, darkly stained nuclei and minimal cytoplasm, consistent with lymphocytes, located between adipose tissue (white vacuolated cells) and skeletal muscle (pink striated fibers). The second cell type, eosinophils, exhibited distinct morphological features including eosinophilic granules, bilobed nuclei, and red-stained cytoplasm, especially visible under Giemsa staining (Figure 6A). Notably, eosinophils were only abundantly distributed within the inflamed areas in the OVA + um-V2 and OVA + 2m'-V3 groups (indicated by red arrows). Manual quantification using ImageJ revealed a significant increase in the percentage of eosinophils within the infiltrate in the OVA+um-V2 and OVA+2m'-V3 groups, when compared to the negative control, OVA-alone, and other two methylated ODN groups (Figure 6B). Notably, eosinophil percentages closely mirrored the serumIL-5 levels observed in each group, suggesting that elevated IL-5 expression drives these eosinophilic infiltrations.

3.6. Unmethylated um-V2 Strongly Induces Nucleic Acid-Sensing TLRs In Vitro Mouse Splenocytes

To explore potential mechanisms underlying the differential immunological effects of CpG ODNs, we examined the expression of nucleic acid-sensing Toll-like receptors (TLRs) in mouse splenocytes in vitro under ODNs treatment. Specifically, we assessed TLR7 and TLR8, which

 doi:10.20944/preprints202506.1691.v1

recognize single-stranded RNA, and TLR9, which detects DNA. Splenocytes isolated from a single untreated BALB/c mouse were cultured with 25µg of unmethylated uM-V2, methylated 2m-V1, or alternate methylated 2m'-V3 for 2 and 6 hours. RNA was extracted and compared with PBS-treated controls.

At the 2-hour time point, methylated 2m-V1 induced a ~15-fold increase inTLR7 expression compared to PBS. However, by 6 hours, splenocytes treated with unmethylated um-V2 showed markedly elevated expression of all three TLRs, with nearly a 50-fold increase in TLR9, a 4.5-fold increase in TLR8, and a 4-fold increase in TLR7. These levels were significantly higher than those observed in any other treatment group. In contrast, both methylated 2m-V1 and 2m'-V3 did not induce notable changes in TLR expression at this time point. This expressional data suggest that unmethylated um-V2 robustly activates nucleic acid-sensing TLRs, particularly TLR9, while methylated CpG ODNs may evade detection through these canonical pathways.

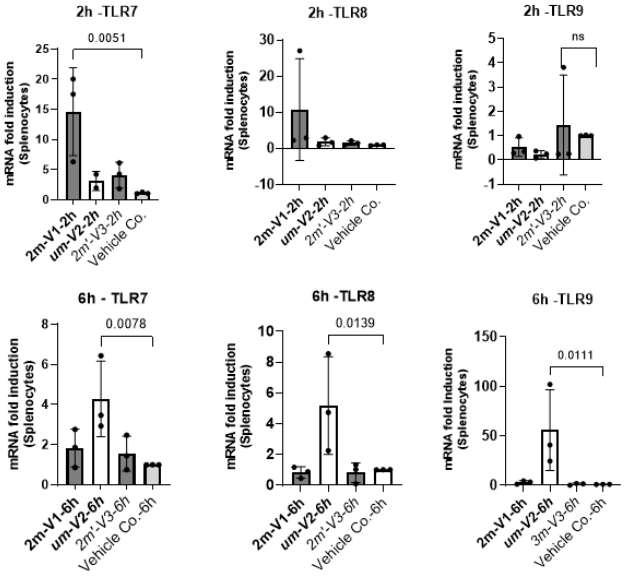

Figure 7. Differential expression of nucleic acid-sensing TLRs in mouse splenocytes challenged with methylated and unmethylated ODNs in vitro. Mouse splenocytes were cultured in vitro and treated with 25µg of unmethylated UM-V2, methylated 2M-V1, or alternatively methylated 2M'-V3. Total RNA was extracted at 2hours (top panel) and 6hours (bottom panel) post-treatment, reverse transcribed to cDNA, and analyzed by RT-qPCR forthe expression of TLR-7, TLR-8, and TLR-9. Gene expression levels were calculated as fold changes relative to the PBS control after normalization to the ΔCt of internal GAPDH gene. Bar plots display mean fold changes with statistical comparisons performed using one-way ANOVA. Significant differences ($p<0.05$) are indicated; non-significant comparisons are not labeled.

4. Discussion

This study demonstrates that methylation status and sequence type of CpG ODNs profoundly influence allergic responses in an OVA-induced mouse model. Among the tested sequences, methylated 3m-V4 and 2m-V1 ODNs consistently exhibited immunomodulatory effects that attenuate Th2/Th17-driven allergic inflammation.

First, both methylated 3m-V4 and 2m-V1 significantly suppressed serum anti-OVA IgE levels and mitigated allergic symptoms, indicating a protective role in IgE-mediated hypersensitivity. This suppression aligns with their capacity to counteract the OVA-induced reduction in $CD4^+$ T cells, suggesting a broader immune-restorative function. Importantly, the increase in $CD4^+CD25^+FOXP3^+$ Treg cells, coupled with reductions in Th2 and Th17 subsets, points to a shift toward immune

 doi:10.20944/preprints202506.1691.v1

tolerance. This shift is likely mediated through regulatory circuits that counterbalance the pro-inflammatory milieu typically driven by IL-4 and IL-5 in allergic contexts.

Consistent with this, serum cytokine profiling revealed elevated IL-10 levels in 3m-V4- and 2m-V1-treated mice, supporting their anti-inflammatory effect. In contrast, co-administration of um-V2 or methylated 2m'-V3 intensified the allergic response, as evidenced by increased IL-4, IL-5, and eosinophilic infiltration at the injection site. These contrasting profiles suggest that not all CpG ODNs are beneficial in allergy modulation and that sequence-specific and methylation-dependent factors critically shape their outcomes.

The marked local skin inflammation observed in the um-V2 and 2m'-V3 groups further reinforces their pro-allergic potential. The associated eosinophil accumulation is consistent with the elevated IL-5 levels, underscoring a Th2-skewed response by them[17]. In contrast, the immunosuppressive effect of 3m-V4 and 2m-V1 may reflect a context-dependent induction of regulatory pathways, which is well know to override the allergen-induced immune deviation [18–20].

To further explore the underlying mechanisms, we examined the expression of nucleotide-sensing Toll-like receptors (TLRs) in splenocytes following in vitro ODN exposure. Unmethylated DNA activates TLR9 is primarily known for its pro-inflammatory role [21,22]. However, recent research highlights TLR9 capacity to dampen inflammation in certain contexts. For example, TLR9 and downstream target, IFN-α, are required for the migration of myeloid-derived suppressor cells into gastric tissue to suppress the establishment of persistent H. pylori infection [23]. While methylated 2m-V1 induced minimal TLR expression in this study, unmethylated um-V2 triggered striking upregulation of TLR9 (~50-fold), TLR8 (~4.5-fold), and TLR7 (~4-fold) at 6 hours. These results in the same line of literatures suggest that unmethylated ODNs robustly engage canonical nucleic acid-sensing pathways, particularlyTLR9, which may also account for their pro-inflammatory and Th2-skewing effects observed in our in vivo model. Conversely, the limited TLR induction by methylated ODNs implies alternative recognition pathways, such as self-DNA sensing the cGAS-STING pathway) [24] or reduced engagement with TLR-expressing immune subsets. Although these in vitro data are preliminary, this differential TLR engagement may contribute to the distinct immunological profiles observed in vivo.

The natural origin of this set of CpG ODNs from a probiotic bacterial genome supports their potential safety for use in human allergic disease. The differential immunomodulatory effects observed among the four ODN variants in this study clearly underscore the importance of both methylation status and the precise positioning of methylated cytosine(s) in the design of anti-allergic DNA vaccines. The opposing roles of 2m-V1 and um-V2 on Treg induction, previously reported, were reaffirmed in this study. Furthermore, the inclusion of two newly tested methylated variants—2m'-V3 and 3m-V4—provided additional insights. Notably, 2m'-V3, despite containing two methylated cytosines and having similar structural stability to 2m-V1, exhibited a Treg/Teff response pattern more closely resembling that of the unmethylated um-V2. This suggests that the precise position of methylation in 2m-V1 is critical for its immunomodulatory effect. Moreover, 3m-V4, which contains three methylated sites, demonstrated superior anti-allergic efficacy compared to 2m-V1, offering a promising example of how methylation density and placement can be optimized to enhance therapeutic outcomes. These findings provide a valuable framework for refining the design of methylated ODN-based vaccines by strategically tailoring their methylation patterns.

In summary, our findings support the therapeutic potential of selected methylated CpG ODNs, especially 3m-V4 and 2m-V1, in mitigating allergic inflammation. By dampening IgE responses, enhancing Treg populations, and avoiding over activation of nucleic acid-sensing TLRs, these ODNs may help restore immune balance. Further studies are warranted to dissect the TLR-independent mechanisms potentially activated by methylated DNA sequences and to assess their translational relevance in human allergy models.

5. Conclusions

 doi:10.20944/preprints202506.1691.v1

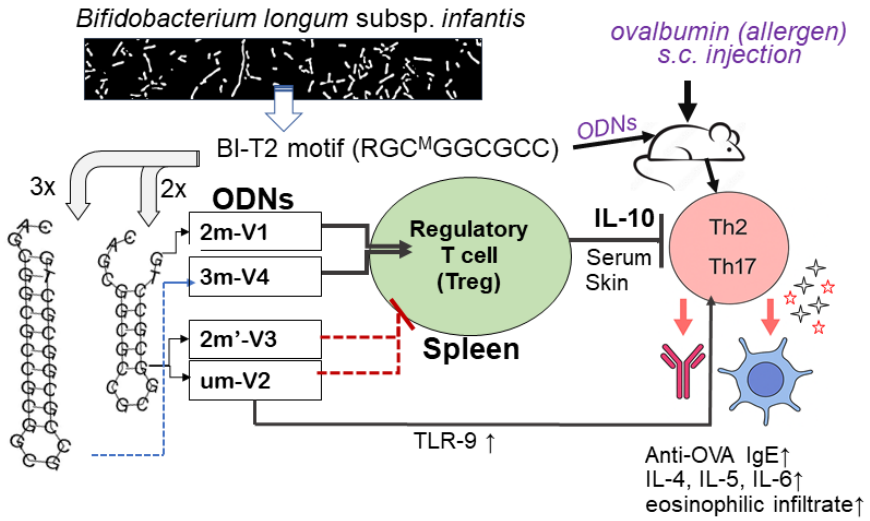

Figure 8. Caption.

Supplementary Materials: The following supporting information can be downloaded at the website of this paper posted on Preprints.org, Figure S1: Schematic gate strategy.

Author Contributions: Conceptualization, Dongmei Li, Idalia Cruz and Joseph Bellanti; Data curation, Samantha Peltak; Formal analysis, Joseph Bellanti; Investigation, Dongmei Li and Idalia Cruz; Methodology, Samantha Peltak; Resources, Patricia Foley; Writing – original draft, Joseph Bellanti; Writing – review & editing, Dongmei Li and Idalia Cruz.

Funding: This research received no external funding.

Institutional Review Board Statement: The animal study protocol was approved by the the Institutional Animal Care and Use Committee (IACUC) of Georgetown University (Protocol #2022-0021)and date of 2022 July 1st for studies involving animals.

Informed Consent Statement: Not applicable for studies not involving humans.

Data Availability Statement: Not applicable.

Acknowledgments: Not applicable.

Conflicts of Interest: The authors declare no conflicts of interest.

Abbreviations

The following abbreviations are used in this manuscript:

ODN	oligodeoxynucleotides
OVA	ovalbumin
CpG	cytosine-phosphate-guanine
AIC	immunotherapy
Treg	regulatory T cells
um-V2	unmethylated CpG oligodeoxynucleotide
2m-V1	CpG oligodeoxynucleotide incorporating two 5-methylcytosines at positions 4 and 12
2m´-V3	CpG oligodeoxynucleotide with two 5-methylcytosines shifted at positions 7 and 15
3m-V4	CpG oligodeoxynucleotide with an extended backbone structure, with three 5-methylcytosines at positions 3, 11 and 19

References

 doi:10.20944/preprints202506.1691.v1

1. Krieg, A.M.; Yi, A.K.; Matson, S.;Waldschmidt, T.J.; Bishop, G.A.; Teasdale, R.;Koretzky, G.A.;Klinman D.M. CpG motifs in bacterial-DNA trigger direct B-cell activation. *Nature***1995**, *374*(6522):546–549. doi: 10.1038/374546a0.
2. Salem, A.K.; Weiner, G.J. CpG oligonucleotides as immunotherapeutic adjuvants: innovative applications and delivery strategies. *Adv. Drug Deliv. Rev.***2009**, *61*(3):193-4. doi: 10.1016/j.addr.2008.12.003
3. Jacquet, A. Nucleic acid vaccines and CpG oligodeoxynucleotides for allergen immunotherapy. *Curr. Opin. Allergy. Clin. Immunol.***2021**, *21*(6):569-575. doi: 10.1097/ACI.0000000000000772.
4. Montamat, G.; Leonard, C.;Poli, A.; Klimek, L.;Ollert, M. CpG Adjuvant in allergen-specific immunotherapy: finding the sweet spot for the induction of immune tolerance. *Front. Immunol*. **2021**, *12*:590054. doi: 10.3389/fimmu.2021.590054
5. Hemmi, H.; Takeuchi, O.; Kawai, T.;Kaisho,T.;, Sato S.;Sanjo, H. A Toll-like receptor recognizes bacterial DNA. *Nature***2000**, *408*(6813):740–745. doi:10.1038/35047123
6. Marabelle, A.;Kohrt, H.;Sagiv-Barfi, I.;Ajami, B.; Axtell, R.C.; Zhou, G.; Rajapaksa, R.; Green, M.R.; Torchia, J.; Brody, J.; Luong, R.; Rosenblum, M.D.; Steinman, L.;Levitsky, H.I.;Tse, V.; Levy R. Depleting tumor-specific Tregs at a single site eradicates disseminated tumors. *J. Clin. Invest.***2013**, *123*(6):2447-63. doi: 10.1172/JCI64859. Erratum in*: J Clin Invest*. 123(11):4980.
7. Sellars, M.C.; Wu, C.J.; Fritsch,E.F.. Cancer vaccines: building a bridge over troubled waters. *Cell***2022**, *185*(15):2770-2788. doi: 10.1016/j.cell.2022.06.035.
8. Liu, W.; Yang, X.; Wang, N.; Fan, S.; Zhu, Y.; Zheng, X.; Li Y. Multiple immunosuppressive effects of CpG-c41 on intracellular TLR-mediated inflammation. *Mediators Inflamm*. **2017**,*2017*:6541729. doi: 10.1155/2017/6541729.
9. Li, Y.; Cao, H.; Wang, N.; Xiang, Y.; Lu, Y.; Zhao, K.; Zheng, J.; and Zhou, H. A novel antagonist of TLR9 blocking all classes of immunostimulatory CpG-ODNs.*Vaccine*. **2011**.29: 2193–2198, https://doi.org/10.1016/j.vaccine.2010.10.042
10. Krieg A.M.. CpG motifs in bacterial DNA and their immune effects. *Annu. Rev. Immunol*. **2002**, *20*:709–760. doi: 10.1146/annurev.immunol.20.100301.064842
11. Klinman, D.M.; Currie, D.;Gursel, I.;Verthelyi, D. Use of CpG oligodeoxynucleotides as immune adjuvants. *Immunol. Rev*. **2004**,*199*:201–216. doi:10.1111/j.0105-2896.2004.00161.x
12. Bellanti, J.A., and Li, D. Treg cells and epigenetic regulation. *Adv. Exp. Med. Biol*. **2021**,*1278*:95-114. doi: 10.1007/978-981-15-6407-9_6.
13. Li, D.; Cheng, J.; Zhu, Z.;Catalfamo, M.; Lawless, O.J.; Bellanti, J.A. Treg-inducing capacity of genomic DNA of *Bifidobacterium longum* subsp. *infantis*. *Allergy Asthma Proc*. **2020**, *41*(5):372–385. doi:10.2500/aap.2020.41.190099
14. Li, D.; Sorkhabi, S.; Cruz, I.; Foley, P.L.; Bellanti, J.A. Studies of methylated CpG ODN from *Bifidobacterium longum* subsp. *infantis* in a murine model: Implications for treatment of human allergic disease. *Allergy Asthma Proc*. **2025a,** *46*(1):e13–e23. doi:10.2500/aap.2025.46.230013
15. Li, D.; Cruz, I.;Sorkhabi, S.; Foley, P.L.; Bellanti, J.A. Dose-response studies of methylated and nonmethylated CpG ODNs from Bifidobacterium longum subsp. infantis for optimizing Treg cell stimulation. *Allergy Asthma Proc*. **2025b,** *46*(2):98–104. doi:10.2500/aap.2025.46.240021
16. Lawless, O.J.; Bellanti, J.A.; Brown, M.L.; Sandberg, K.;Umans, J.G.; Zhou, L.; Chen, W.; Wang, J.; Wang, K.; Zheng, S.G. In vitro induction of T regulatory cells by a methylated CpG DNA sequence in humans: Potential therapeutic applications in allergic and autoimmune diseases. *Allergy Asthma Proc*. **2018**, *39*(2):143–152. doi:10.2500/aap.2018.39.4124
17. Spencer, L.A.; Weller, P.F. Eosinophils and Th2 immunity: contemporary insights. *Immunol Cell Biol.***2010**, *88*(3):250-6. doi: 10.1038/icb.2009.115.
18. Robinson, D.S.;Larché, M.; Durham, S.R. Tregs and allergic disease. *J Clin Invest.***2004**,*114*(10):1389-97. doi: 10.1172/JCI23595.
19. Palomares, O.;Yaman, G.;Azkur, A.K.;Akkoc, T.;Akdis, M.;Akdis, C.A. Role of Treg in immune regulation of allergic diseases. *Eur. J. Immunol*. **2010**, *40*(5):1232-40. doi: 10.1002/eji.200940045. PMID: 20148422.
20. Akdis, C.A.;Akdis,M.. Mechanisms of immune tolerance to allergens: role of IL-10 and Tregs. *J Clin Invest*. **2014**, *124*(11):4678-80. doi: 10.1172/JCI78891.

 doi:10.20944/preprints202506.1691.v1

21. Dalpke, A.; Frank, J.; Peter, M.;Heeg, K. Activation of toll-like receptor 9 by DNA from different bacterial species. *Infect. Immun.***2006**, *74*(2):940-6. doi: 10.1128/IAI.74.2.940-946.2006.
22. Kou M.; Wang, L. Surface toll-like receptor 9 on immune cells and its immunomodulatory effect. *Front. Immunol*. **2023**, *14*:1259989,
23. Varga, M.G.;Piazuelo, M.B., Romero-Gallo J., Delgado A.G., Suarez G., Whitaker M.E., Krishna U.S., Patel R.V., Skaar E.P., Wilson K.T., Algood H.M. Peek R.M. Jr. TLR9 activation suppresses inflammation in response to Helicobacter pylori infection. Am. J. Physiol. Gastrointest. *Liver Physiol*. **2016**, *311*(5):G852-G858. doi: 10.1152/ajpgi.00175.2016.
24. Ma, R.; Ortiz Serrano T.P.; Davis, J.;Prigge, A.D.; Ridge, K.M. The cGAS-STING pathway: The role of self-DNA sensing in inflammatory lung disease. *FASEB J.***2020**, *34*(10):13156-13170. doi: 10.1096/fj.202001607R.